



Advances in the Theory of Nonlinear Analysis and its Applications

ISSN: 2587-2648

Peer-Reviewed Scientific Journal

Efficient spectral Legendre Galerkin approach for the advection diffusion equation with constant and variable coefficients under mixed Robin boundary conditions

Zineb Laouar^a, Nouria Arar^b, Talaat Abdelhamid^c

^aLaboratoire des Mathématiques Appliquées et Didactique, Ecole Normale Supérieure El Katiba Assia Djebar, Constantine, Algeria. Centre Universitaire Abdelhafid Boussouf, Mila, Algeria.

^bLaboratoire des mathématiques et sciences de la décision (LAMASD), Université Frères Mentouri, Constantine, Algeria.

^cShenzhen Institutes of Advanced Technology, Chinese Academy of Sciences, Shenzhen, China.

Physics and Mathematical Engineering Department, Faculty of Electronic Engineering, Menoufiya University, Menouf, Egypt.

Abstract

This paper aims to develop a numerical approximation for the solution of the advection-diffusion equation with constant and variable coefficients. We propose a numerical solution for the equation associated with Robin's mixed boundary conditions perturbed with a small parameter ε . The approximation is based on a couple of methods: A spectral method of Galerkin type with a basis composed from Legendre-polynomials and a Gauss quadrature of type Gauss-Lobatto applied for integral calculations with a stability and convergence analysis. In addition, a Crank-Nicolson scheme is used for temporal solution as a finite difference method. Several numerical examples are discussed to show the efficiency of the proposed numerical method, specially when ε tends to zero so that we obtain the exact solution of the classic problem with homogeneous Dirichlet boundary conditions. The numerical convergence is well presented in different examples. Therefore, we build an efficient numerical method for different types of partial differential equations with different boundary conditions.

Email addresses: z.laouar@centre-univ-mila.dz (Zineb Laouar), arar.nouria@umc.edu.dz (Nouria Arar), talaat.2008@yahoo.com (Talaat Abdelhamid)

Received July 6, 2022; Accepted: December 27, 2022; Online: January 4, 2023.

Keywords: Spectral method Galerkin's method Robin's conditions Advection-Diffusion equation Gauss-Quadrature Difference scheme Crank Nicolson scheme.
2010 MSC: 65N06, 65N22, 65N35, 33C45.

1. Introduction

The advection and diffusion are two processes of significant importance in the real world applications. They describe a physical phenomena where the transport of particles such as mass, energy, heat, humidity, pollutant, etc. The Advection-Diffusion equation has several engineering applications such as the heat transfer, water transfer in soils, chemical engineering, biosciences, velocity, vorticity, dispersion of tracers in porous media, etc [1, 2, 3, 4]. This equation is used to describe the transport of air and groundwater pollutants, the contaminant or pollutant concentration distribution behaviour through air, rivers, lakes and porous medium like aquifer. In this study, we consider a model of advection-diffusion equation in the form

$$\frac{\partial u}{\partial t}(t, x) + a(x) \frac{\partial u}{\partial x}(t, x) - b(x) \frac{\partial^2 u}{\partial x^2}(t, x) = f(t, x), \quad (1)$$

where $x \in [-1, 1]$, $t > 0$ and the coefficients of advection and diffusion are $a(x)$ and $b(x)$, respectively, and defined in $\mathcal{C}^1([-1, 1])$. The initial condition is $u(0, x) = g(x)$ and boundary conditions are of type Robin perturbed with a parameter $\varepsilon > 0$ such that

$$\begin{aligned} u(t, -1) - \varepsilon \frac{\partial u}{\partial x}(t, -1) &= 0, \\ u(t, 1) + \varepsilon \frac{\partial u}{\partial x}(t, 1) &= 0. \end{aligned}$$

This equation has been solved using many numerical methods specially when the boundary conditions are from Dirichlet or Neumann types, conditions of Robin type which consider a linear combination between the function and its derivative, are used to modelise important and vital problems of chemical engineering and heat transfer. Mojtabi and Deville [5] considered the time dependent one-dimensional linear advection-diffusion equation with Dirichlet homogeneous boundary conditions. They observed that when the advection becomes dominant, the analytical solution becomes ill-behaved and harder to evaluate.

The numerical simulation became very useful, easier and more efficient in time and results specially for time-dependent problems. Hutomo et al. [6] studied the numerical solution of the advection-diffusion equation with variable coefficient. The obtained results from the Du-Fort Frankel method for the 2-D advection-diffusion equation have agreement with that of the analytical solution. Abdelhamid et al. [7, 8], solved the heat conduction problem using the continuous linear finite element method and applied the backward difference scheme in the time discretization. Abdelhamid et al. [9] used the mixed finite element technique to solve the forward problem of elasticity with using the Galerkin method and the weighted residual method is applied to the linear elasticity problem. Ma et al. [10] applied the Chebyshev-Galerkin and Chebyshev collocation methods to solve the two-dimensional Helmholtz model equation. Balyan et al. [11] presented a pseudospectral method to solve Fisher's equation in 1D and 2D using Chebyshev-Gauss-Lobatto points and collocation in the spatial and the temporal directions.

In this paper, we propose a spectral method to approximate the solution of the advection-diffusion equation with Robin's boundary conditions. The approximation is based on using a special basis consisting of a certain linear combination of Legendre polynomials that satisfy boundary conditions [12, 13, 14]. Spectral methods use basically orthogonal polynomials (Legendre, Chebyshev, ...) [15, 16], this relation is one from advantages of Sturm-Liouville problems [17, 18]. In fact, spectral approximation of the solution of an evolution problem is regarded as a finite expansion of eigenfunctions of a suitable Sturm-Liouville problem and since the most common eigenfunctions are polynomials we choose orthogonal once for their several properties depending on the interval of study $[-1, 1]$, (see [12, 19]). The importance of this kind of eigenfunctions problems is to guarantee spectral accuracy comparing to finite differences and finite elements methods [10, 13, 14]. To get

the best results from spectral method, specially when calculating integrals, we introduce a Gauss-Quadrature method using Legendre-Gauss-Lobatto nodes and their correponding weights. Due to their high accuracy, Gauss formulas play fundamental role in the theoretical analysis of spectral methods. The possibility of integrating polynomials just by knowing their values at M points will be widely used, in addition, the fact that the points $x = -1$ and $x = 1$ are included in the nodes is very important for imposed boundary conditions [17, 19]. Analytical results in the form of stability and convergence theorems are also derived in this study to investigate and reinforce the property of spectral accuracy [11, 20]. Moreover the temporal solution of the problem is established using a Crank-Nicolson scheme with an appropriate temporal step [21]. In this study, we seek for taking the advantage of Legendre polynomials, Gauss-quadratures to apply Galerkin and Crank-Nicolson methods, so we obtain the best approximate solution of the advection-diffusion problem.

2. Preliminaries

Let $I = [-1, 1]$, $L^2(I)$ is the space of measurable function v on I such that $\|v\| < +\infty$. The scalar product and the L^2 norm are respectively defined by

$$\langle u, v \rangle = (u, v)_{L^2} = \int_I u(x)v(x) dx; \quad \|v\|_{L^2}^2 = (v, v)_{L^2}.$$

For every positive m , the Sobolev space is defined by

$$H^m(I) = \left\{ v; \frac{\partial^k v}{\partial x^k} \in L^2(I), \quad 0 \leq k \leq m \right\},$$

and the standard semi-norm and norm are

$$|v|_{L^2(I)} = \left\| \frac{\partial v}{\partial x} \right\|_{L^2(I)}, \quad \|v\|_{H^m} = \sum_{k=0}^m \left\| \frac{\partial^k v}{\partial x^k} \right\|_{L^2(I)}.$$

We denote by \mathbb{P}_N the space of polynomials of degree less than or equal to N . Let $L_N(x), x \in I$ be the standard Legendre polynomial of degree N . The family of Legendre polynomials $\{L_k(x)\}_{k \in \mathbb{N}}$ constitutes a Hilbert basis of $L^2(I)$ and they are solutions of the following differential Legendre equation [17, 18]

$$(1 - x^2) L_N''(x) - 2xL_N'(x) + N(N + 1) L_N(x) = 0, \quad N \geq 0.$$

They satisfy the recurrence relation

$$(1 - x^2)L_N'(x) = -NxL_N(x) + NL_{N-1}(x),$$

and the Rodrigues formula

$$L_N(x) = \frac{(-1)^N}{2^N N!} \frac{d^N}{dx^N} (1 - x^2)^N.$$

The polynomial $L_N(x)$ is of degree N , for all $N \in \mathbb{N}$ and the coefficient of its highest degree term is $\frac{(2N)!}{2^N (N!)^2}$.

They also satisfy the relation of orthogonality relative to the weight $w(x) = 1$ in $[-1, 1]$

$$\forall N \neq M \in \mathbb{N}, \quad \int_{-1}^1 L_N(x)L_M(x) dx = 0 \quad \text{and} \quad \int_{-1}^1 L_N^2(x) dx = \frac{2}{2N + 1}.$$

The first Legendre polynomials are given by

$$\begin{aligned} L_0(x) &= 1, & L_1(x) &= x, & L_2(x) &= (3x^2 - 1)/2, \\ L_3(x) &= (5x^3 - 3x)/2, & L_4(x) &= (35x^4 - 30x^2 + 3)/8. \end{aligned}$$

In particular, we have

- $L_N(1) = 1, \quad L_N(-x) = (-1)^N L_N(x), \quad L_N(-1) = (-1)^N.$
- $L'_N(1) = \frac{N(N+1)}{2}, \quad L'_N(-1) = \frac{N(N+1)}{2}(-1)^{N+1}.$

We give also some other properties of Legendre polynomials

- $\forall x \in I, \quad |L_N(x)| \leq 1,$
- $\forall x \in I, \quad |L'_N(x)| \leq \frac{N(N+1)}{2},$
- $(N + 1) L_{N+1}(x) = (2N + 1)x L_N(x) - N L_{N-1}(x).$

3. The model problem

Consider the following problem

$$\begin{cases} \frac{\partial u}{\partial t}(t, x) + a(x) \frac{\partial u}{\partial x}(t, x) - b(x) \frac{\partial^2 u}{\partial x^2}(t, x) = f(t, x), & -1 < x < 1, \quad t > 0, \\ u(t, -1) - \varepsilon \frac{\partial u}{\partial x}(t, -1) = 0, & t > 0, \\ u(t, 1) + \varepsilon \frac{\partial u}{\partial x}(t, 1) = 0, & t > 0, \end{cases} \tag{2}$$

where ε is a small parameter in $(0, 1]$ and $u(0, x) = g(x)$ is a given initial condition. We focus on the case where the advection and diffusion coefficients are defined functions in $C^1(I)$. Let $a(x) \geq 0$ and $b(x) > 0, \forall x \in I$. Multiplying the equation of problem (2) by w which depends only on x , and integrating by parts, we obtain

$$\begin{aligned} \int_{-1}^1 \frac{\partial u}{\partial t} w(x) \, dx + \int_{-1}^1 b(x) \frac{\partial u}{\partial x} \frac{dw}{dx} \, dx + \int_{-1}^1 (a(x) + b'(x)) \frac{\partial u}{\partial x}(t, x) w(x) \, dx \\ = \int_{-1}^1 f(t, x) w(x) \, dx + \left[b(x) \frac{\partial u}{\partial x}(x) w(x) \right]_{-1}^1. \end{aligned} \tag{3}$$

The boundary conditions give

$$\frac{\partial u}{\partial x}(-1) = \frac{u(-1)}{\varepsilon}, \quad \frac{\partial u}{\partial x}(1) = -\frac{u(1)}{\varepsilon}.$$

Hence the weak formulation of the problem (2) is

$$\begin{cases} \text{Find } u(t) \in H^1(I), \text{ such that} \\ \frac{d}{dt} \langle u(t), w \rangle + r(u(t), w) = \langle f(t), w \rangle \end{cases} \tag{4}$$

with an initial condition $u(0, x) = g(x)$ and where

$$\begin{aligned} r(u(t), w) = \int_{-1}^1 b(x) \frac{\partial u}{\partial x}(t, x) \frac{dw}{dx}(x) \, dx + \int_{-1}^1 (a(x) + b'(x)) \frac{\partial u}{\partial x}(t, x) w(x) \, dx \\ + \frac{1}{\varepsilon} (b(1)u(t, 1)w(1) + b(-1)u(t, -1)w(-1)). \end{aligned} \tag{5}$$

Theorem 3.1. *Let $T > 0$ be a final time and an initial data $g \in L^2(I)$.*

The following problem with the bilinear form $r(u(t), w)$ defined in (5)

$$\begin{cases} \frac{d}{dt} \langle u(t), w \rangle + r(u(t), w) = \langle f(t), w \rangle, & \forall w \in H^1(I), \quad 0 < t < T, \\ u(t = 0) = g(x), \end{cases} \tag{6}$$

has a unique solution $u \in L^2(]0, T[; H^1(I)) \cap \mathcal{C}([0, T]; L^2(I))$.

Proof. The idea of this proof is in [21].

It is clear that $r(\cdot, \cdot)$ is a symmetric bilinear form. So, we prove the continuity and coercivity to ensure the existence and the uniqueness of the solution. The continuity is ensured by using the Cauchy-Schwarz inequality and the fact that

$$|u(\pm 1)| \leq \sup |u(x)| = \|u\|_{L^\infty(I)}, \quad \forall x \in I.$$

So, we obtain

$$\exists \delta > 0, \quad \forall u(t), w \in H^1(I) \quad \|r(u(t), w)\| \leq \delta \|u(t)\|_{H^1(I)} \|w\|_{H^1(I)},$$

such that $\delta = \left(1 + \frac{2}{\varepsilon} B_+ + A_+ + B'_+\right)$, where for all $x \in I$, we have

$$A_+ = \max a(x) \geq 0, \quad B_+ = \max b(x) > 0, \quad B'_+ = \max |b'(x)|.$$

The weak coercivity is also ensured, we have

$$r(u(t), u(t)) + \frac{A_-}{2} \|u\|_{L^2(I)}^2 \geq B_- \left\| \frac{\partial u}{\partial x} \right\|_{L^2(I)}^2 + \frac{B'_-}{2} (u^2(1) - u^2(-1)).$$

So, we obtain the existence of $M = \min(B_-, 1)$ and $\eta = \left(\frac{A_- + B'_-}{2} + 1\right)$, where for all $x \in I$, we have

$$A_- = \min a(x) \geq 0, \quad B_- = \min b(x) > 0, \quad B'_- = \min |b'(x)|.$$

Then

$$r(u(t), u(t)) + \eta \|u(t)\|_{L^2(I)}^2 \geq M \|u(t)\|_{H^1(I)}^2, \quad \forall u(t) \in H^1(I).$$

Hence, the existence and the uniqueness of the solution of the problem (4) is proved. □

4. Construction of numerical approximation

4.1. Spatial Discretization

We define $W_N \subset H^1(I)$ as

$$W_N = \{w \in \mathbb{P}_N \text{ such that } w(-1) - \varepsilon w'(-1) = 0 \text{ and } w(1) + \varepsilon w'(1) = 0\}.$$

The Legendre spectral scheme for (4) is

$$\begin{cases} \text{Find } u_N(t) \in W_N, \text{ such that} \\ \frac{d}{dt} \langle u_N(t), w_N \rangle + r(u_N(t), w_N) = \langle f(t), w_N \rangle, \quad \forall w_N \in W_N. \end{cases} \quad (7)$$

We choose as a basis of W_N a family of polynomials constructed from orthogonal Legendre polynomials defined by [22, 23]

$$\psi_k(x) = \gamma_k (L_k(x) + \alpha_k L_{k+1}(x) + \beta_k L_{k+2}(x)), \quad k = 0, \dots, N - 2, \quad (8)$$

where α_k, β_k , and γ_k are coefficients determined when $\{\psi_k\}$ verify the boundary conditions of the problem (2) and $\|\psi_k(x)\| = 1$, (see [14, 22]). By a simple calculation and using the properties of Legendre polynomials we obtain for $\varepsilon > 0$ and $k = 0, \dots, N - 2$

$$\begin{aligned} \alpha_k &= 0, \quad \beta_k = -\frac{1 + \varepsilon k(k+1)/2}{1 + \varepsilon(k+2)(k+3)/2}, \\ \gamma_k &= \left(\frac{2}{2k+1} + \beta_k^2 \frac{2}{2k+5} \right)^{-1/2}. \end{aligned} \quad (9)$$

We denote the approximate solution by $u_N(t, x)$ defined as

$$u_N(t, x) = \sum_{k=0}^{N-2} u_k(t) \psi_k(x). \tag{10}$$

By substituting (10) in (7), we obtain the following scheme

$$\frac{d}{dt} \sum_{k=0}^{N-2} u_k(t) \langle \psi_k, \psi_j \rangle + \sum_{k=0}^{N-2} u_k(t) r(\psi_k, \psi_j) = \langle f(t), \psi_j \rangle, \quad \forall j = 0, \dots, N-2,$$

such that

$$\begin{aligned} \langle \psi_k, \psi_j \rangle &= \int_{-1}^1 \psi_k(x) \psi_j(x) dx, \\ r(\psi_k, \psi_j) &= \int_{-1}^1 b(x) \psi'_k(x) \psi'_j(x) dx + \int_{-1}^1 (a(x) + b'(x)) \psi'_k(x) \varphi_j(x) dx, \\ &\quad + \frac{1}{\varepsilon} (b(1) \psi_k(1) \psi_j(1) + b(-1) \psi_k(-1) \psi_j(-1)), \\ \langle f(t), \psi_j \rangle &= \int_{-1}^1 f(t, x) \psi_j(x) dx. \end{aligned}$$

To approximate this calculations and guarantee spectral accuracy, we use an integration formula of type Gauss-Lobatto based on Legendre-Gauss-Lobatto (LGL) nodes with their corresponding weights [17, 18, 19], characterized by the following formula for p polynomial of N degree, η_i the LGL nodes and w_i the corresponding weights.

$$\int_{-1}^1 pw dx = \sum_{i=0}^N p(\eta_i^{(N)}) w_i^{(N)}.$$

We obtain the matrix form (11) for $U(t) = (u_0, u_1, \dots, u_{N-2})^T$

$$\frac{d}{dt} \mathbf{A}U(t) + \mathbf{B}U(t) = \mathbf{C}(t), \tag{11}$$

such that \mathbf{A} and \mathbf{B} are $(N-1) \times (N-1)$ matrices

$$\begin{aligned} \mathbf{A}_{k,j} &= [\langle \psi_k, \psi_j \rangle]_{0 \leq k, j \leq N-2}, \quad \mathbf{B}_{k,j} = [r(\psi_k, \psi_j)]_{0 \leq k, j \leq N-2}, \\ \mathbf{C}(t) &= (C_0, \dots, C_{N-2})^T \text{ where } C_j = \langle f(t), \psi_j \rangle \text{ for } j = 0, \dots, N-2. \end{aligned}$$

4.2. Time Discretization

Now we use a Crank-Nicolson scheme, the U_i^n represents the solution of U at node η_i and time t_n (the η_j discretize in the range $[-1, 1]$ with the LGL nodes and $\Delta t > 0$ discretize in $[0, T]$). We obtain the following scheme

$$\begin{aligned} \left(\mathbf{A} + \frac{\Delta t}{2} \mathbf{B} \right) U_i^{n+1} &= \left(\mathbf{A} - \frac{\Delta t}{2} \mathbf{B} \right) U_i^n + \frac{\Delta t}{2} (\mathbf{C}(t_n) + \mathbf{C}(t_{n+1})), \\ U_i^0 &= g(\eta_i), \end{aligned} \tag{12}$$

where $g(\eta_i)$ is the value of $g(x)$ at each node η_i of the discretization $[-1, 1]$.

5. Stability and convergence analysis

In this section, we set up the stability and convergence results for the Legendre-Galerkin spectral method in order to achieve the spectral accuracy. The theorems are obtained following the same idea in chapter 6 from [24].

Theorem 5.1. *There exists a positive constant C independent of N such that the solution u_N of (7) satisfies the following estimate*

$$\|u_N(t)\|_{L^2(I)}^2 + K \int_0^t \|u_N(s)\|_{L^2(I)}^2 ds \leq \|u_N(0)\|_{L^2(I)}^2 + C \int_0^t \|f(s)\|_{L^2(I)}^2 ds. \tag{13}$$

Proof. By setting $w_N = u_N$ in (7) we get

$$\frac{1}{2} \frac{d}{dt} \|u_N(t)\|_{L^2(-1,1)}^2 + r(u_N(t), u_N(t)) = \langle f(t), u_N(t) \rangle. \tag{14}$$

Since $r(.,.)$ is only weakly coercive then there exists $K > 0$ such that $K|u|_{H^1(I)}^2 \leq r(u, u), \forall u \in H^1(I)$ where $|u|_{H^1(I)}$ is the semi norm on $H^1(I)$.

Using this inequality in (14) we obtain

$$\frac{1}{2} \frac{d}{dt} \|u_N(t)\|_{L^2(-1,1)}^2 + K \|u_N(t)\|_{L^2(-1,1)}^2 \leq \|f(t)\|_{L^2(I)} \|u_N(t)\|_{L^2(I)}. \tag{15}$$

Now throughout Young inequality we obtain

$$\frac{d}{dt} \|u_N(t)\|_{L^2(I)}^2 + K \|u_N(t)\|_{L^2(I)}^2 \leq \frac{1}{K} \|f(t)\|_{L^2(I)}^2. \tag{16}$$

Integrating the last estimate for $t \geq 0$ we obtain the desired estimate which ensures the stability since $\frac{1}{K}$ is independent of N with $u_N(0) = g(x)$. □

Passing to the convergence analysis, we first need to set some definitions.

Let's define the error function between the solution $u_N(t)$ of the scheme (7) and the exact solution of (4) as $E(t) = R_N u(t) - u_N(t)$

where R_N is the projection defined by $R_N : H^1(I) \rightarrow W_N$ such that for $N \rightarrow \infty$,

$$\|u - R_N u\|_{H^1(I)} \rightarrow 0 \text{ for all } u \in H^1(I).$$

Let be $u \in L^2(I)$, we define the norm of u in the dual space of $H^1(I)$ noted $(H^1(I))^*$ by

$$\|u\|_{(H^1(I))^*} = \sup_{v \in H^1(I)} \frac{\langle u, v \rangle}{\|v\|}, \quad v \neq 0.$$

And we have

$$\|u\|_{(H^1(I))^*} \leq C \|u\|_{L^2(I)}.$$

Theorem 5.2. *Let $u(t)$ be the exact solution of (4) and $u_N(t)$ the solution of (7), the following estimate holds*

$$\begin{aligned} & \|E(t)\|^2 + K \int_0^t |E(s)|_{H^1(I)}^2 ds \leq \|E(0)\|^2 \\ & + C \left(\int_0^t \left\| \frac{\partial u}{\partial t}(s) - R_N \frac{\partial u}{\partial t}(s) \right\|_{(H^1(I))^*} ds + \int_0^t \|(u - R_N u)(s)\|_{H^1(I)} ds \right), \end{aligned} \tag{17}$$

where C is a constant independent of N .

Proof. $E(t)$ satisfy the following estimate using the weak corecivity of $r(.,.)$

$$\frac{1}{2} \frac{d}{dt} \|E(t)\|^2 + K |E(t)|_{H^1(I)}^2 \leq \left| \left\langle \frac{\partial u}{\partial t} - R_N \frac{\partial u}{\partial t}, e \right\rangle + r(u - R_N u, e) \right| \tag{18}$$

Using the above definitions and the continuity of the form $r(.,.)$ we obtain the existence of a constant C independant of N such that

$$C \|E(t)\|_{H^1(I)} \left(\left\| \frac{\partial u}{\partial t} - R_N \frac{\partial u}{\partial t} \right\|_{(H^1(I))^*} + \|u - R_N u\|_{H^1(I)} \right) \tag{19}$$

By replacing this result in (18), an error bound is estimated when integration for all $t \geq 0$, We conclude that the approximation is convergent. \square

6. Numerical results

To test the performance of the described spectral method, we propose the following examples, where we solve numerically the problem (2) and show the convergence of the approximation to the analytical solution of the problem with boundary conditions of type Dirichlet when ε reaches zero. All the computations are carried out in double precision using Matlab 9.8.0 (R2020a). Executions were done on AMD Ryzen 5 5600X 6-Core, 3.70Ghz Desktop. The figures are obtained for $N_x = 20$ nodes of LGL in domain $[-1, 1]$ and 100 subdivision of temporal domain. The approximation error in the case where we don't know the exact solution (i.e. when $\varepsilon \neq 0$) is calculated for ε fixed using the formula

$$err = \|u_N - u_{N+2}\|_\infty \quad N = 2, 4, \dots, 2n, \dots; \quad n \geq 1. \tag{20}$$

The exact solution of the Dirichlet boundary problem is known and in order to compare it to the numerical solution, maximum error (\mathcal{E}_{max}), square error (\mathcal{E}_{sq}) and relative error norms (\mathcal{E}_{re}) are calculated as follows

$$\mathcal{E}_{max} = \|u_{exact} - u_N\|_\infty = \max_i |(u_{exact})_i - (u_N)_i|, \quad i = 1, 2, \dots, N_x; \tag{21}$$

$$\mathcal{E}_{sq} = \|u_{exact} - u_N\|_2 = \left[\Delta x \sum_{i=1}^{N_x} |(u_{exact})_i - (u_N)_i|^2 \right]^{1/2}; \tag{22}$$

$$\mathcal{E}_{re} = \|u_{exact} - u_N\|_R = \frac{\|u_{exact} - u_N\|_2}{\|u_{exact}\|_2}. \tag{23}$$

Example 6.1. In equation (2) let $a(x) = a = 0.01$, $b(x) = b = 1$, $T = 1$ with the initial condition

$$u(0, x) = \cos\left(\frac{\pi}{2}x\right)$$

and

$$f(t, x) = \left(\left(b \frac{\pi^2}{4} - 1 \right) \cos\left(x \frac{\pi}{2}\right) + a \frac{\pi}{2} \sin\left(x \frac{\pi}{2}\right) \right) \exp(-t).$$

For homogeneous Dirichlet boundary conditions, the exact solution is given by

$$u(t, x) = \exp(-t) \cos\left(\frac{\pi}{2}x\right).$$

Figure 1 shows the convergence of the approximate to the exact solution at different ε , where $\varepsilon = 0.2, 0.1, 0.02, 0.01, 0.001$. When ε tends to zero, the approximate solution gets closer to the exact one from Dirichlet boundary conditions.

The variations of the error of the approximate solution (err) are presented in Figure 2. It is observed that the error of the approximate solution decreases with increasing N .

In Figure 3 we can compare the exact solution of the problem with homogeneous Dirichlet boundary conditions with the approximative solution obtained using the approximative method when $\varepsilon = 10^{-8}$ and $N = 10$.

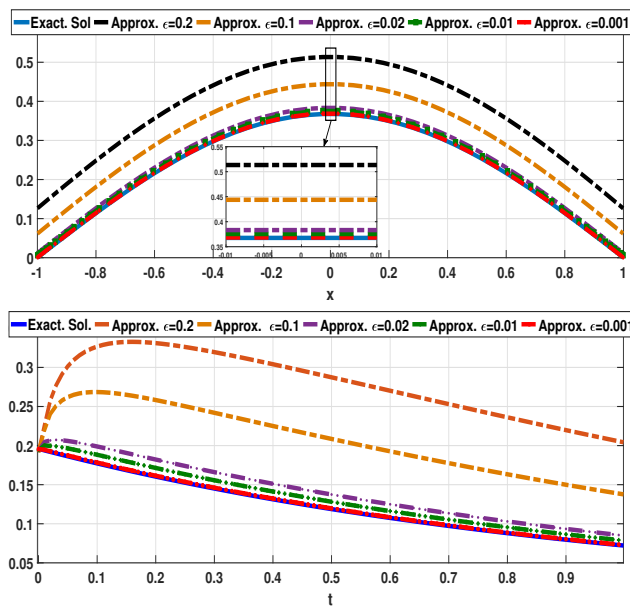


Figure 1: The behavior of the approximate solution when ε tends to 0 at $N = 10$ for fixed $t = 1$ (up) and for fixed $x = -0.874$ (down)

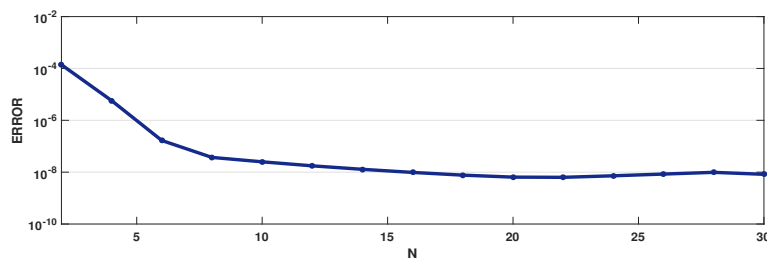


Figure 2: Logarithmic approximation error as a function of N at $\varepsilon = 10^{-8}$ for Example 6.1

Example 6.2. We assume that in (2) $a(x) = a = 0, b(x) = b = 1, T = 1$, the initial condition and the term f defined as

$$u(0, x) = \cos\left(\frac{\pi}{2}x\right), \quad f(t, x) = 0.$$

For homogeneous Dirichlet boundary conditions, the exact solution is given by

$$u(t, x) = \cos\left(\frac{\pi}{2}x\right) \exp\left(-\frac{b\pi^2}{4}t\right).$$

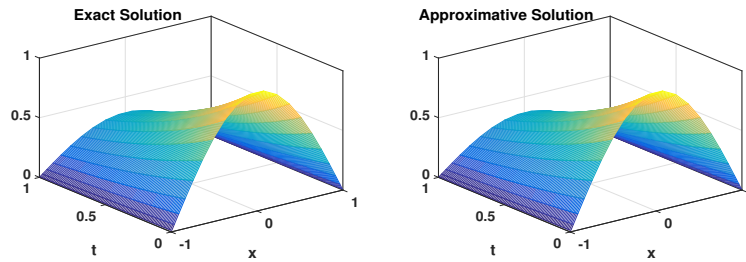


Figure 3: Representation of the exact solution for the problem with Dirichlet boundary conditions and the approximate solution at $N = 8$ and $\varepsilon = 10^{-8}$ for Example 6.1

Figure 4 shows the exact and the obtained approximate solution for different N . It presents the convergence of the approximation for different N , where $N = 6, 8, 10$ and $\varepsilon = 10^{-2}, 10^{-3}, 10^{-4}$ at $x = 0.227$ and $t = 1$. In each case, an error value is given calculated using the appropriate ε and N . The obtained results show the convergence of the approximate solution of (2) when ε tends to 0 to the exact solution of Dirichlet boundary conditions problem.

Table 1 gives the square error norm \mathcal{E}_{sq} calculated for different values of N .

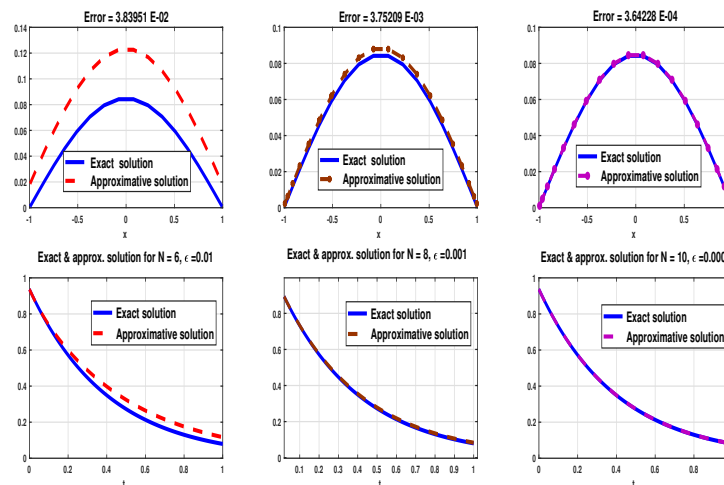


Figure 4: The behavior of exact and approximate solution for different N and ε with the appropriate \mathcal{E}_{sq} for fixed $t = 1$ (up) and fixed $x = 0.227$ (down) for Example 6.2

Table 1: Error values as a function of N for $\varepsilon = 10^{-8}$ for Example 6.2.

N	\mathcal{E}_{sq}
4	6.46185e – 05
8	8.93058e – 06
12	8.93059e – 06
16	8.92040e – 06
20	8.86360e – 06

Example 6.3. Let $a(x) = a = 0.09$, $b(x) = b = 2$, $T = 1$, the initial condition

$$u(0, x) = 0$$

and

$$f(t, x) = \left(2t + b\pi^2 \frac{t^2}{4}\right) \cos\left(x \frac{\pi}{2}\right) + a\pi \frac{t^2}{2} \sin\left(x \frac{\pi}{2}\right).$$

For homogeneous Dirichlet boundary conditions, the exact solution is given by

$$u(t, x) = t^2 \cos\left(x \frac{\pi}{2}\right).$$

Figure 5 shows the convergence of the approximate solution with decreasing ε upto $\varepsilon = 0.001$. When ε takes the values 0.08, 0.05, 0.025, 0.001 the curve of the approximation for a fixed x or a fixed t gets closer to the curve of the exact solution of the Dirichlet boundary conditions problem. This result is well shown in Table 2 in which the error is calculated for different N . For $\varepsilon = 10^{-8}$, the numerical solution is very close to the exact solution. Table 3 introduces the \mathcal{E}_{re} at $N = 4, 8$ and 10 of different LGL nodes in $[-1, 1]$.

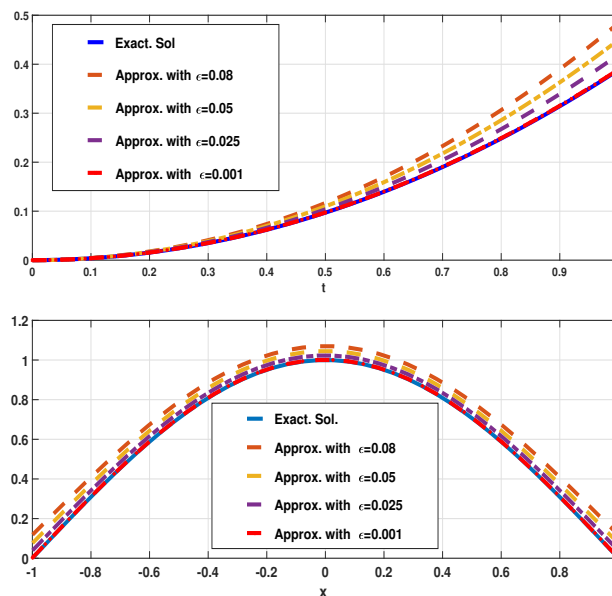


Figure 5: The exact solution compared to the approximate solution for different ε with $N = 10$, for fixed $x = -0.281$ (up) and fixed $t = 1$ (down) for Example 6.3

Table 2: Error values as a function of N for $\varepsilon = 10^{-8}$ for Example 6.3.

N	\mathcal{E}_{sq}	N	\mathcal{E}_{sq}
4	9.22208e - 04	14	8.74526e - 06
6	1.36494e - 04	16	6.03520e - 06
8	5.11646e - 05	20	2.77529e - 06
10	2.46797e - 05	24	1.68477e - 06
12	1.39021e - 05	30	8.29894e - 07

Example 6.4. Let $a(x) = a = 0$, $b(x) = 1 - x^2$, $T = 1$ with the initial condition given by

$$u(0, x) = x \cos\left(x \frac{\pi}{2}\right)$$

Table 3: Relative error \mathcal{E}_{re} for different N when $\varepsilon = 10^{-8}$ for Example 6.3.

x	$N = 4$	$N = 8$	$N = 10$
-0.944	7.51812e - 03	6.43507e - 04	3.26354e - 04
-0.755	1.14864e - 03	2.38689e - 05	4.65406e - 05
-0.458	2.60600e - 04	3.26515e - 06	3.28677e - 05
-0.095	9.29549e - 04	3.15130e - 05	1.86307e - 05
0.281	4.41661e - 04	5.66697e - 05	1.39810e - 05
0.617	2.32730e - 03	6.63974e - 05	2.60646e - 05
0.865	8.60915e - 04	2.34344e - 04	4.61786e - 06

and

$$f(t, x) = \exp(t) \left(\left(x + \frac{\pi^2}{4} x(1 - x^2) \right) \cos\left(x \frac{\pi}{2}\right) + \left(\frac{-a\pi}{2} x + \pi(1 - x^2) \right) \sin\left(x \frac{\pi}{2}\right) \right).$$

The exact solution for the Dirichlet boundary conditions problem is

$$u(t, x) = x \exp(t) \cos\left(x \frac{\pi}{2}\right).$$

Table 4 presents the \mathcal{E}_{max} and \mathcal{E}_{sq} for the decreased ε when $N = 10$. Table 5 exposes the relative error calculated in different nodes for $N = 4, 8$ and 12 , the results are obtained for $\varepsilon = 10^{-8}$ to show the convergence of the approximation to the exact solution of the problem with Dirichlet boundary conditions when ε reaches 0.

Table 4: Error values for different ε at $N = 10$ for Example 6.4.

ε	\mathcal{E}_{sq}	\mathcal{E}_{max}
10^{-1}	9.05505e - 01	1.03184e + 00
10^{-2}	2.91516e - 01	3.25393e - 01
10^{-3}	3.62864e - 02	4.05446e - 02
10^{-4}	3.73871e - 03	4.17051e - 03
10^{-5}	3.75677e - 04	4.18251e - 04
10^{-6}	3.81611e - 05	4.18316e - 05
10^{-7}	4.45936e - 06	4.17778e - 06
10^{-8}	1.28603e - 06	1.28416e - 06
10^{-10}	1.02004e - 06	1.11888e - 06

Table 5: Relative error values \mathcal{E}_{re} for different N when $\varepsilon = 10^{-8}$ for Example 6.4.

x	$N = 4$	$N = 8$	$N = 12$
-0.912	1.46648e - 01	4.52127e - 05	2.29492e - 06
-0.510	1.51450e - 03	1.44248e - 05	1.33381e - 06
0.076	5.97860e - 02	2.44510e - 05	1.22646e - 06
0.227	4.95987e - 02	9.91097e - 06	1.24621e - 06
0.746	7.19953e - 02	2.44251e - 06	1.55148e - 06

Example 6.5. Assume that $a(x) = 1 - x^2$, $b(x) = b = 2$, $T = 1$ with the initial condition

$$u(0, x) = (1 - x^2) \sin\left(x \frac{\pi}{2}\right)$$

and

$$f(t, x) = \exp\left(\frac{-\pi^2}{4}t\right) \left(\left((1-x^2)\left(\frac{-\pi^2}{4} - 2x + b\frac{\pi^2}{4}\right) + 2b \right) \sin\left(x\frac{\pi}{2}\right) + \left(\frac{\pi}{2}(1-x^2)^2 + 2b\pi x\right) \cos\left(x\frac{\pi}{2}\right) \right).$$

The exact solution for the problem with Dirichlet boundary conditions is given by

$$u(t, x) = \exp\left(\frac{-\pi^2}{4}t\right) (1-x^2) \sin\left(x\frac{\pi}{2}\right).$$

Figure 6 is obtained using different decreasing values of ε . Noting that when ε tends to 0 the obtained approximation is so close to the exact solution for the problem with Dirichlet boundary conditions. Tables

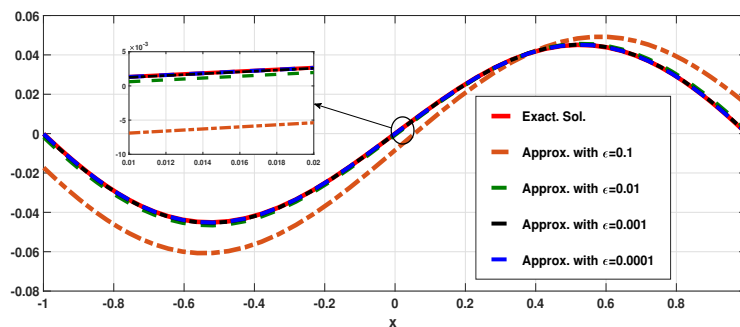


Figure 6: Exact and approximate solution for different ε at $N = 10$ and $t = 1$ for Example 6.5

6 shows the error calculated at different ε . It is observed that with increasing N , the approximate solution is more interesting comparing to the exact one. This approach investigates the numerical convergence of the obtained approximate solution at the Dirichlet boundary conditions when ε tends to 0. Figure 7 compares

Table 6: Error values for different values of N when $\varepsilon = 10^{-8}$.

N	\mathcal{E}_{sq}	\mathcal{E}_{max}
4	3.86296e - 03	4.19989e - 03
6	3.98687e - 04	4.56514e - 04
8	1.26445e - 04	1.50269e - 04
10	6.06861e - 05	7.60106e - 05
12	3.39352e - 05	3.93346e - 05
14	2.12362e - 05	2.51413e - 05
16	1.45927e - 05	1.74079e - 05
20	6.52682e - 06	7.32607e - 06

the exact solution of the Dirichlet boundary conditions problem and the approximate one obtained using the proposed numerical method at $N = 10$ and $\varepsilon = 10^{-8}$. Figure 8 illustrates also the exact solution of Dirichlet boundary conditions, the obtained approximation and the absolute error. By taking a new step of discretization for the temporal domain $\Delta t = 0.001$, the results of convergence stay the same.

7. Conclusion

In this study, the advantages of Legendre polynomials with its important properties and Gauss quadratures are established to build an approximation of the advection-diffusion solution. The proposed numerical

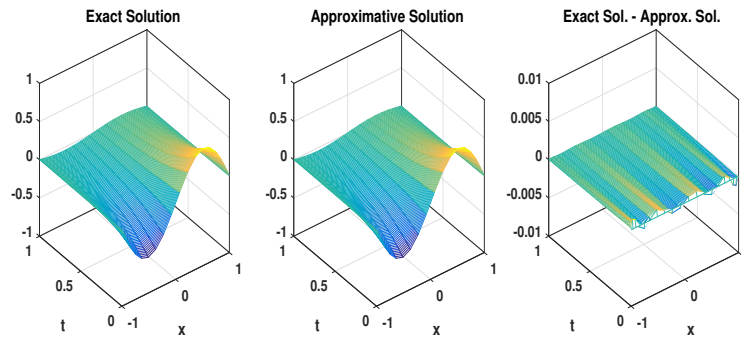


Figure 7: Representation of the exact solution of Dirichlet boundary conditions problem, the approximate solution obtained using the described method and the difference for $N = 10$ and $\varepsilon = 10^{-8}$ for Example 6.5

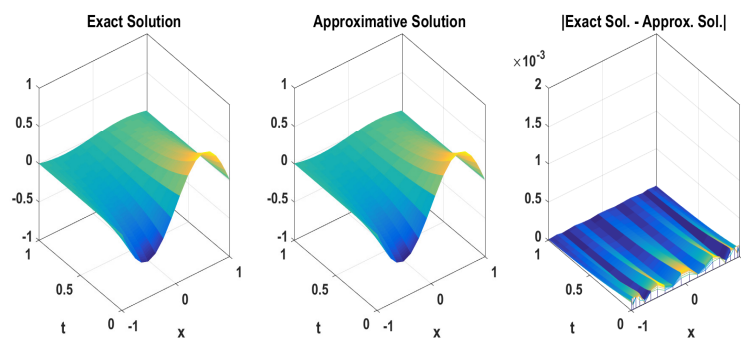


Figure 8: Representation of the exact solution of Dirichlet boundary conditions problem, the approximate solution obtained using the described method and the absolute error for $N = 16$, $\varepsilon = 10^{-8}$ and $\Delta t = 0.001$ for Example 6.5

approach is presented in two steps: first, we defined the basis used in Galerkin approximation and the type of Gauss quadrature is used to obtain the exact calculation of integrals. Secondly, a Crank-Nicolson scheme is developed to solve the obtained system depending on the time variable. The stability and the convergence analysis of the method are also proved by giving an estimation depending on the initial values for the stability and an error bound that characterizes the convergence. Several examples of different cases are presented with various types of results to prove the numerical convergence of the approximate solution to the exact one with Dirichlet boundary conditions, when ε tends to zero. The obtained results are introduced and interpreted in different error types (the \mathcal{E}_{re} , \mathcal{E}_{sq} and \mathcal{E}_{max}). The obtained results show that the introduced method is efficient and can be used to solve many time-dependent problems of different partial differential equations with different types of boundary conditions. The proposed approach enjoys the spectral accuracy that is with small data we can reach a high precision of the approximation which has been illustrated by several numerical examples.

Acknowledgments

Z. Laouar and N. Arar acknowledge support from Directorate General for Scientific Research and Technological Development (DGRSDT), Algeria. The work of Talaat Abdelhamid is supported by Science, Technology & Innovation Funding Authority (STDF) under grant number 39385.

Conflict of interest

The authors declare no potential conflict of interests.

References

- [1] J. Isenberg, C. Gutfinger, Heat transfer to a draining film, *Int. J. Heat Trans.* 16 (1973) 505-512.
- [2] J.Y. Parlange, Water transport in soils, *Ann. Rev. Fluids Mech* 2 (1980) 77-102.
- [3] P.C. Chatwin, C.M. Allen, Mathematical models of dispersion in rivers and estuaries, *Ann. Rev. Fluids Mech* 17 (1985) 119-149.
- [4] N. Kumar, Unsteady flow against dispersion in finite porous media, *J Hydrol* 63 (1998) 345-358.
- [5] A. Mojtabi, M.O. Deville, One-dimensional linear advection–diffusion equation: Analytical and finite element solutions, *Computers & Fluids* 107 (2015) 189-195.
- [6] G.D. Hutomo, J. Kusuma, A. Ribal, A.G Mahie, N. Aris, Numerical solution of 2-d advection-diffusion equation with variable coefficient using du-fort frankel method, *J Physics: Conf. Series* 1180 (2019) 012009.
- [7] T. Abdelhamid, A.H. Elsheikh, A. Elazab, S.W. Sharshir, E.S. Selima, D. Jiang, Simultaneous reconstruction of the time-dependent Robin coefficient and heat flux in heat conduction problems, *Inverse Problems in Science and Engineering* 26(9) (2018) 1213-1248.
- [8] T. Abdelhamid, A.H. Elsheikh, O.M. Omisore, N.A. Saeed, T. Muthuramalingam, R. Chen, M.M. Alam, Reconstruction of the heat transfer coefficients and heat fluxes in heat conduction problems, *Mathematics and Computers in Simulation* 187 (2021) 134-154.
- [9] T. Abdelhamid, R. Chen, M.M. Alam, Nonlinear conjugate gradient method for identifying Young's modulus of the elasticity imaging inverse problem, *Inverse Problems in Science and Engineering* 29(12) (2021) 2165-2185.
- [10] X. Ma, Y. Wang, X. Zhu, W. Liu, W. Xiao, Q. Lan, A High-Efficiency Spectral Method for Two-Dimensional Ocean Acoustic Propagation Calculations, *Entropy* 23(9) (2021) 1227.
- [11] L.K. Balyan, A.K. Mittal, M. Kumar, M. Choube, Stability analysis and highly accurate numerical approximation of fisher's equations using pseudospectral method, *Mathematics and Computers in Simulation* 117 (2020) 86-104.
- [12] F. Jędrzejewski, *Introduction aux méthodes numériques*. Deuxième édition, Springer-Verlag, Paris, France (2005).
- [13] A. Quarteroni, C. Canuto, M.Y. Hussaini, T.A. Zang, *Spectral methods in fluid dynamics*, Springer-Verlag, Berlin, Heidelberg, (1988).
- [14] J. Shen, T. Tang, L. Wang, *Spectral methods, algorithms, analysis and applications*, Springer-Verlag, Berlin, Heidelberg, (2011).
- [15] D. Gottlieb, S. Orszag, *Numerical Analysis of Spectral Methods: Theory and Applications*, SIAM, Philadelphia, (1977).
- [16] M.H. Carpenter, D. Gottlieb, Spectral methods on arbitrary grids, *Journal of Computational Physics* 129(1) (1996) 74-86.
- [17] D. Funaro, *Polynomial approximation of differential equations*, Springer-Verlag, Berlin, Heidelberg, (1992).
- [18] B.C. Carlson, *Special functions of applied mathematics*, Academic Press, New York, (1978).
- [19] A. Quarteroni, R. Sacco, F. Saleri, *Méthodes numériques. Algorithmes, analyse et application*, Springer-Verlag, Milano, Italia, (2004).
- [20] A. Chattouh, K. Saoudi, Error analysis of Legendre-Galerkin spectral method for a parabolic equation with Dirichlet-Type non-local boundary conditions, *Mathematical Modelling and Analysis* 26(2) (2021) 287-303.
- [21] G. Allaire, *Analyse numérique et optimisation*, Edition de l'école polytechnique, (2007).
- [22] J. Shen, Efficient spectral-Galerkin method I. Direct solvers for the second and fourth order equations using Legendre polynomials, *SIAM Journal on Scientific Computing* 15 (1994) 1489-1505.
- [23] J. Shen, Efficient Chebyshev-Legendre Galerkin methods for elliptic problems, *Proceedings of the third international conference on spectral and high order methods*, *Houston Journal of Mathematics* 70(34) (1998) 233-239.
- [24] A. Quarteroni, C. Canuto, M.Y. Hussaini, T.A. Zang, *Spectral methods, fundamentals in single domains*, Springer-Verlag, Berlin Heidelberg, (2006).